PDK4-Mediated Metabolic Reprogramming Promotes Rituximab Resistance in Diffuse Large B-Cell Lymphoma Via Negative Regulation of MS4A1/CD20

Duanfeng Jiang
Central South University Third Xiangya Hospital
Qiuyu Mo
Guilin Medical University Affiliated Hospital
Xiaoying Sun
Qinghai Provincial People's Hospital
Xiaotao Wang
Guilin Medical University Affiliated Hospital
Min Dong
The Second Affiliated Hospital of Nanjing University of Chinese Medicine
Guozhen Zhang
Guilin Medical University Affiliated Hospital
Fangping Chen
Central South University Third Xiangya Hospital
Qiangqiang Zhao (zgxyws@163.com)
Central South University Third Xiangya Hospital

Research

Keywords: PDK4, diffuse large B-cell lymphoma, MS4A1/CD20, rituximab, metabolic reprogramming

Posted Date: May 17th, 2021

DOI: https://doi.org/10.21203/rs.3.rs-490131/v1

Abstract

Background: Diffuse large B cell lymphoma (DLBCL) heterogeneity promotes the recurrence and anti-CD20-based therapeutic resistance. In previous studies, it has been demonstrated that the downregulation of MS4A1/CD20 expression after chemoimmunotherapy with rituximab can lead to rituximab resistance. However, the the mechanisms of CD20-loss remains unknown.

Methods: The expression levels of PDK4 were investigated in DLBCL patients and cell lines by RNA-seq, qRT-PCR, western blotting and immunofluorescence analysis. Lentiviral infection was used to regulate the level of PDK4 in DLBCL cells. The effects of PDK4 on apoptosis, drug sensitivity and proliferation of DLBCL cells were evaluated by flow cytometry and cell-counting kit-8 (CCK-8) assay, as well as being assessed in a murine model. Cell metabolism was conducted by measurement of glucose consumption, lactate production, ATP levels, ECAR and OCR with corresponding assay kit.

Results: Our data showed that PDK4 expression levels elevated significantly in DLBCL cells derived from both the patients and cell lines with rituximab plus cyclophosphamide, doxorubicin, vincristine, and prednisone regimen) resistant. We further found that the overexpression of PDK4 in DLBCL cells can lead to cell proliferation and rituximab resistance both *in vitro* and *in vivo*. Furthermore, the loss of PDK4 expression or treatment with the PDK4 inhibitor dichloroacetate is effective in increasing the rituximab-induced cell apoptosis in DLBCL cells. According to the mechanism studies, PDK4 mediated a metabolic shift that the main energy source was changed from OXPHOS to glycolysis. More importantly, with the knockdown or overexpression of PDK4 in DLBCL cells leads to a reverse MS4A1/CD20 expression.

Conclusion: Our data identify a metabolic reprogramming role of PDK4 in rituximab resistance of DLBCL and highlight the unique function of PDK4 as an attractive therapeutic target.

Background

As the most common lymphoid malignancy, diffuse large B-cell lymphoma (DLBCL) comprises a heterogeneous group with pathophysiological, genetic and clinical characteristics[1]. Most of the patients can be cured with rituximab plus cyclophosphamide, doxorubicin, vincristine, and prednisone regimen (R-CHOP), which is the current standard regimen[2]. In spite of this, approximately 40% of the patients with DLBCL still suffer therapeutic failure with R-CHOP[3-5], which underlines the necessity to identify molecular for providing new prognostic biomarkers and/or therapeutic targets.

The molecular heterogeneity of DLBCL is considered to be a major influencing factor in the response to R-CHOP therapy[6]. The cell-of-origin (COO) classification and the consensus cluster classification (CCC) capture clearly different molecular aspects of DLBCL. The COO classification elaborates on the subgroups of DLBCL into distinct transcriptional profiles: activated B-cell-like (ABC), germinal-center B-cell-like (GCB), and unclassified[7]. The CCC identifies vrious DLBCL subsets including the BCR/proliferation cluster (BCR-DLBCL), the oxidative phosphorylation (OxPhos) cluster (OxPhos-DLBCL)

and the host response (HR) tumors[8]. The nutrient and energy metabolism in OxPhos-DLBCL are characterized by elevated oxidative phosphorylation and the increased contribution of mitochondria to total cellular energy budget, while the “non-OxPhos” DLBCLs show greater glycolytic flux[9]. However, it remains unknown whether distinct metabolic fingerprints would affect DLBCL response to R-CHOP. DLBCL represents the highly metabolically active tumors previously treated with R-CHOP regimen[10]. Therefore, targeting DLBCL metabolic specificity might be an effective therapeutic approach in clinic practice, especially for R-CHOP low responder patients.

Rituximab, a chimeric monoclonal antibody targeted against the pan-B-cell marker CD20[11], has been demonstrated as capable to be activated by rituximab binding to CD20 following complement-dependent cytotoxicity (CMC), antibody-dependent cellular cytotoxicity (ADCC) and apoptosis[12-14]. However, the loss of CD20 is a major obstacle to the re-treatment of relapsed/refractory DLBCL with rituximab-based regimens[15]. MS4A1, which encodes CD20, experiences rarely nonsense and missense mutations in newly diagnosed samples. However, these mutations increase significantly after rituximab-associated therapy[16]. In addition, the occurrence of CD20 down-regulation has been observed in a number of patients developing resistant to rituximab-based therapies, which has been proven as one of the most significant causes for rituximab resistance[17-19]. Therefore, it is believed that understanding the mechanisms of CD20-loss phenotype could promote the development of solutions to rituximab resistance in DLBCL.

Metabolic reprogramming plays an essential role in tumour progression and drug resistance in various cancers [10, 20-22]. As a variety of PDK isozyme, pyruvate dehydrogenase lipoamide kinase isozyme 4 (PDK4) is expressed at high levels in cardiac and skeletal muscle, in addition to being overexpressed in various tumors[23]. The upregulation of pyruvate dehydrogenase kinase family (PDK1-4) is associated with aerobic glycolysis and chemoresistance through the inhibition of the pyruvate dehydrogenase complex (PDH)[24]. PDK4 has been suggested as one of the most significant influencing factors in cell metabolism by directing carbon flux into glycolysis from OXPHOS[25,26]. Most recently, DLBCL has been demonstrated as being characterize by metabolic heterogeneity in different subtypes and different periods of therapy[9,10]. However, there is still no investigation conducted into the effects of metabolic shift and its related mechanisms in rituximab resistance of DLBCL.

So far, the role played by PDK4 in DLBCL is still not clarified. In this study, PDK4 was identified as most upregulated in rituximab-resistant DLBCL cells. It was further discovered that PDK4 promoted the growth of DLBCL cells both *in vitro* and *in vivo*, and that the elevated expression of PDK4 in DLBCL patients exerted a negative regulatory effect on MS4A1/CD20 expression. In terms of the mechanism, PDK4-mediated metabolic shift was associated with the mechanism by which PDK4 induced cell growth and rituximab resistance in DLBCL. As suggested by these results, PDK4 promoted DLBCL cell growth and rituximab resistance by partially regulating MS4A1/CD20 expression, to say the least.

Materials And Methods

Patients and tissue samples

The study was granted approval from the Ethics Committee of the Third Xiangya Hospital of Central South University. In accordance with the Declaration of Helsinki, informed consent was obtained from the patients. Both tissue samples and clinical data were obtained from the patients diagnosed with DLBCL before treatment between December 2018 and August 2020. The diagnosis of DLBCL was confirmed by at least two pathologists in line with the World Health Organization classification[27]. After collection, the tissues were immediately frozen and stored in liquid nitrogen. Cryopreserved tissues contained both cancerous and paired distant normal tissues. This study was carried out in a retrospective series of 56 DLBCL cases with cryopreserved tissues, with follow-up lasting until December 2020.

Cell culture and reagents

The human DLBCL cell lines U2932, OCI-ly7 and OCI-ly8, and human normal B-lymphocyte cell line GM12878 were provided by the Cancer Research Institute of Central South University. The human DLBCL cell line SU-DHL-2 and the R-CHOP-resistant DLBCL cell line SU-DHL-2/R were sourced from Xiangya Hospital of Central South University and then characterized as reported previously[28]. All of the cell lines were cultured in RPMI 1640 (Gibco) with 12% foetal bovine serum, 100 U/mL penicillin and 100 mg/mL streptomycin.

Rituximab-resistant DLBCL cell line OCI-ly8/R was established as previously reported[29]. OCI-ly8 cells were exposed to rituximab for weeks to obtain rituximab-resistant lines. In brief, sensitive parental cell lines were cultured in RPMI-1640 and the cells were exposed to an increasing dose of rituximab for 24 hours immediately after the log phase of growth was reached (from 0.1 to 128 μg/mL). After 24 hours of incubation with rituximab, the cells were centrifuged and recultured in fresh RPMI 1640. Then, the cells were allowed to redevelop for a minimum of 3 days, and the procedure was repeated for 10 times in total once the log phase of growth was reached. The reagents used include rituximab (Roche Pharma), sodium dichloroacetate (#S8615, Selleckchem), puromycin (#S7417, Selleckchem) and G418 Sulfate (#S3028, Selleckchem).

Cell growth ability assay

For cell growth ability assay, 2000 cells in a 200 μL volume were added per well of a 96-well plate and treated with rituximab (50 μg/ml) for a specified period of time. Countess Automated Cell Counter (Thermo Fisher Scientifc) was applied to evaluate count cells. 100% cell viability was measured at hour 0, while relative cell growth was indicated by the ratio of hour X to hour 0.

Cell viability assay

Cell viability assay was performed using CCK-8 solution (Dojindo, Japan) in line with the manufacturer's instructions. In brief, the cells were seeded in 96-well plates (5×10^3 cells per well) and exposed to rituximab (50 μg/ml) for 48 hours either at increased doses, alone or in combination. CCK-8 assay was

carried out according to the standard procedure and the plate was measured at 450 nm using a microplate reader (PerkinElmer, USA).

Cell apoptosis assay

The cells were harvested after 48 hours of treatment, washed with ice-cold PBS, and re-suspended in 400 µL of binding buffer. Then, 20 µg/mL FITC-Annexin V and 5 µg/mL propidium iodide (BD Biosciences) were added to each sample and incubated for 15 minutes. Flow cytometry (Becton Dickinson, USA) was employed to analyse the stained cells, with apoptotic cells treated as Annexin V-positive cells.

Western blotting

Total proteins were extracted with the assistance of RIPA lysis buffer (NCM Biotech) containing freshly added proteinase inhibitor. Then, the proteins obtained were separated by 10–12 % sodium dodecyl sulphate-polyacrylamide gelelectrophoresis and transferred to 0.22 µm PVDF membranes (Millipore). The membranes were blocked with 5 % skim milk and then incubated with primary antibodies overnight at 4 ºC. The respective horseradish peroxidase-conjugated secondary antibodies were added, and protein signals were detected using enhanced chemiluminescence reagents (Affinity Biosciences). ChemiDox XRS Chemiluminescence imaging system (Bio-Rad Laboratories, USA) was adopted to capture and analyse the developed images. The primary antibodies are detailed as follows: anti-PDK4 (DF7169, Affinity Biosciences, 1:1000), anti-CD20 (DF13319, Affinity Biosciences, 1:1000), anti-β-actin (AF7018, Affinity Biosciences, 1:3000).

real-time quantitative polymerase chain reaction (qRT-PCR)

Total RNA was extracted from tissues and cells using the FastPure Cell/Tissue Total RNA Isolation Kit (Vazyme, Nanjing, China). Then, 2 µg of RNA was converted to cDNA with the HiScript III RT SuperMix for qPCR (+gDNA wiper) Kits (Vazyme) according to the instructions from the manufacturer. Gene expression (mRNA) was analysed using the ChamQ Universal SYBR qPCR Master Mix (Vazyme) and LightCycler 480 real-time PCR instrument (Roche) in a two-step qRT-PCR (95 ºC for 30 s, which is followed by 40 cycles of 95 ºC for 10 s and 60 ºC for 30 s). The specific primers (Supplementary Table S2) were synthesized in the Beijing Genomics Institute. Human B-lymphocyte GM12878 cells were taken as a calibrator. The mRNA relative levels of the target genes were calculated using the $2^{-\Delta\Delta Ct}$ method.

RNA-seq and bioinformatics

Total RNA was derived from the tissues as mentioned above. Total mRNA preparation and sequencing were performed in the Beijing Genomics Institute (BGI, Shenzhen, Guangdong, China)[25,30]. In brief, the quality of the RNA samples was assessed using an Agilent Bioanalyzer (Agilent). cDNA libraries were generated using TruSeq RNA Sample Preparation (Illumina), with each library sequenced using single-reads on a HiSeq2000/1000 (Illumina). The levels of gene expression were measured in RPKM using Cufflinks[31]. Differentially expressed genes (DEGs) were identified using the DESeq2 R package. The

criteria for DEGs were set up as fold change (FC, log2) >2 or <−2, Q-value <0.05, and FDR<0.05. RNA sequencing data was analysed by Partek Inc. (St. Louis, MO).

Determination of glucose consumption, lactate production, and ATP levels

The glucose consumption, lactate production, and ATP level assays were conducted according to the previous study[32]. The cells were cultured for a period of 20 hours. The culture media were then harvested, while the lactate and glucose concentrations were measured using a Lactate Assay kit (BioVision, CA, USA) and glucose assay kit (Sigma-Aldrich), respectively. ATP levels were quantified using a colorimetric ATP Assay Kit (Beyotime, Jiangsu, China) according to the instructions from the manufacturer. In brief, cells were harvested and lysed, which is followed by the mixing of supernatant with luciferase reagent, thus catalyzing the light production from ATP and luciferin. Linearly related to the level of ATP concentration, the emitted light was measured using a microplate luminometer. Protein concentration, as measured using a bicinchoninic acid (BCA) protein assay (Beyotime), was referenced to normalize all lactate, glucose, and ATP measurements.

Analysis of mitochondrial ATP synthesis and energy budget calculations.

The rate of mitochondrial ATP synthesis was determined according to previous description[33]. In brief, 2.5 × 10^5 cells were resuspended in 1 ml of buffer containing 150 mM KCl, 25 mM Tris-HCl, 2 mM EDTA, 0.1% BSA, 10 mM K_3PO_4, 0.1 mM $MgCl_2$, 40 g/ml digitonin, 0.15 mM P_1, P_5-Di (adenosine) pentaphosphate (an inhibitor of adenylate kinase), 10 mM malate, 10 mM pyruvate, and 1 mM ADP, either with or without 1 M oligomycin. The cells were incubated at 37°C for 15 minutes. At 0, 5, 10, and 15 min, 50 µl of aliquots of the reaction mixture were quenched in 450 µl of boiling buffer containing 100 mM Tris-HCl and 4 mM EDTA (pH 7.75) for 2 minutes. Then, the aliquots were diluted 1/10 in the quenching buffer and the quantity of ATP was determined using the colorimetric ATP Assay Kit. The rate of mitochondrial ATP synthesis was calculated on the basis of difference in ATP content in the presence and absence of oligomycin.

As for the calculation of energy budget, the contribution of mitochondria and glycolysis to total cellular ATP was measured as previously reported[9,34]. In brief, oxidative ATP turnover was calculated at a presumed P/O ratio of 2.36, where P represents nmol of ATP produced per nmol of oxygen consumed (O), which was in turn derived from the oligomycin-sensitive proportion of OCR. The contribution of glycolysis to energy budget was calculated at a presumed stoichiometric ratio of 1:1 between glycolytically-derived lactate (as described above) and glycolytically-derived ATP. OCR and lactate measurements were performed over a 2-hour period. For each cell line, nmol of ATP derived from glycolysis or oxidative phosphorylation was then pooled and the contributions to the total ATP production were calculated in percentage.

Measurement of ECAR and OCR

The cells were seeded in a 96-well plate with a density of 5×10^4 cells/well and treatment as indicated. Then, they were treated with ECAR reagents according to the recommendations made by the manufacturer (Abcam, UK). The ECAR measurements were performed at an interval of 5 minutes for a total assay time of 120 minutes in a micro-plate reader system (PerkinElmer), with the excitation and emission wavelengths of 380 and 615 nm used, respectively. The level of OCR was measured in real time using the XF24 extracellular flux analyzer instrument (Seahorse Bioscience, USA) as described previously[9,35]. In brief, the cells were equilibrated with bicarbonate-free RPMI 1640 medium supplemented with 25 mM glucose, 1 mM pyruvate, and 2 mM glutamine and incubated overnight. Three metabolic inhibitors were sequentially loaded at a number of specific time points: 1 μM oligomycin, 0.5 μM FCCP, and a combination of 100 nM rotenone with 100 nM myxothiazol. The level of OCR was measured both at the baseline and after the addition of each reagents.

Lentiviral infection

Two pairs of short hairpin RNA sequences (shRNA1 and shRNA2) targeting human PDK4 were annealed and ligated into the Plk0.1-puro lentiviral vector in line with the manufacturer's instruction. The targeting sequences of PDK4 shRNA-1 and shRNA-2 were determined as 5'-ACTGCAACGTCTCTGAGGTG-3' and 5'-AAGCAGATCGAGCGCTACTC-3', respectively. A scrambled shRNA was applied as a control. HEK293T cells were transfected with 16 μg of plasmid containing the expected construct, 12 μg of packing vector pSPAX2 and 8 μg of envelope vector pMD2G in a 10 cm dish for obtaining lentivirus. After the elapse of 48 hours, the culture supernatant was filtered through the 0.45 μm filter and virus concentrated using the PEG 8000 method. Lymphoma cells were incubated with the virus prepared overnight, and the culture medium was replaced with 5 mL of fresh medium. Then, puromycin (2 μg/mL) was used to select infected cells.

Human PDK4 coding sequence was cloned into the pcDNA3.1 plasmid for the generation of a pcDNA/PDK4 expression plasmid. The pcDNA3.1 was treated as empty vector control for subsequent analysis. In order to generate PDK4 stable over expression cells, the lymphoma cells were transfected with pcDNA/PDK4 or vector control through liposome-mediated transfection. G418 (700 μg/ml) was applied to select the transfected cells. After two weeks of selection, the survived cells were seeded individually into 96-well plate for further expansion. The transfection efficacy was determined by means of RT-qPCR and western blotting analysis.

Immunofluorescence analysis

The cells were collected and placed on glass substrates for 20 minutes of fixing with 4 % paraformaldehyde. Then, the fixed cells were rinsed thrice, permeabilized with 0.1 % Triton X-100 (Sigma, USA) for 15 minutes, and blocked with 5 % BSA in phosphate buffered saline (PBS) for 1 hour at room temperature (15-25 ºC). Afterwards, the cells were incubated overnight at 4 ºC with primary antibody against CD20 (DF13319, Affinity Biosciences, 1: 200) and stained with secondary antibody conjugated with Alexa Fluor 488 goat anti-rabbit (S0018, Affinity Biosciences, 1: 200) for 1 hour at room temperature

in the dark, which is followed by counterstaining with 4',6-diamidino-2-phenylindole (Sigma). After three PBS rinses, the samples were covered with coverslip using Antifade Solution (Solarbio). The images were analysed and captured by confocal fluorescence microscope (Olympus, Japan).

Tumour xenografts in mice

All experiments involving animals were approved by the Institutional Animal Care and Use Committee of Central South University, China. The female B-NDG mice (18–20g, 5–7 weeks old) used in this study were obtained from Jiansu Biocytogen Co., Ltd (Nantong, China) [36-38]. DLBCL xenograft mouse model was constructed through the subcutaneous injection of 1×10^7 PDK4 overexpressing OCI-ly8 cells (OCI-ly8 PDK4 OE) or OCI-ly8 cells transfected with empty vector (OCI-ly8 EV) into the right flank of B-NDG mice. At day 10 after the injection of the DLBCL cells, when the tumours became palpable, half of the mice from both the PDK4 overexpressing group and empty vector group were treated with rituximab (12.5 mg/kg, equivalent to 225-275 μg/mice) injected intraperitoneal on a daily basis for 2 weeks, with PBS injected as the control for the rest half of mice. Calliper measurement was performed to determine the diameter of tumour, and the volume of tumour was calculated using the following formula: $0.5 \times \text{length} \times \text{width}^2$. Tumour volume and body weight were measured every 2 days for the mice. They were sacrificed when the volume of tumour reached 2000 mm^3. Then, the tumors were excised and weighed.

Statistical analysis

Expressed as mean ± standard deviation (SD), all data are representative of at least three separate experiments. SPSS 19.0 Student's t-test was conducted to perform comparison between two independent groups, and the corresponding bar chart or line chart was drawn using GraphPad Prism 7 software. To determine the differences between continuous variables, unpaired t test or the Mann-Whitney U test was carried out. Probability values < 0.05 were treated as statistically significant. The mice were randomly assigned to their groups using the random number table.

Results

Elevated PDK4 expression is associated with R-CHOP resistance in DLBCL cells

The clinical characteristics of patients are detailed in Supplementary Table S1. All of the patients participating in this study were treated with the R-CHOP regimen (rituximab, cyclophosphamide, vincristine, doxorubicin, prednisone) in the primary therapy. The responses to treatment were evaluated by CT scans or PET/CT in line with the response criteria for lymphoma[39]. The DLBCL patients treated with R-CHOP regimen were divided into sensitive (n = 37) and resistant (n = 19) groups according to treatment response. Resistant patients were defined as failing to achieve complete remission or show rapid disease progression (less than 6 months) after 6 to 8 cycles of R-CHOP administration. First of all, the differentially expressed genes (DEGs) between four R-CHOP-sensitive patients and three R-CHOP-

resistance patients were screened by means of RNA-seq analysis. According to the results, the expression of PDK4 was significantly elevated in resistance patients as compared to sensitive patients (Fig. 1A). Moreover, the enhancement of PDK4 expression was observed in the patients with activated B-cell-like (ABC) subgroups (n = 26) relative to the patients with germinal centre B-cell-like (GCB) subgroups (n = 30) of DLBCL (P = 0.037, Fig. 1B). Similarly, it was found out among the 56 patients that PDK4 mRNA expression showed significant difference with higher levels detected in resistant patients (P < 0.001, Fig. 1C). A further investigation was conducted into the levels of MS4A1 mRNA expression in the two groups. However, the data revealed no significant difference between sensitive patients and resistance patients (16.72 ± 2.58 vs 15.73 ± 1.80, P = 0.063; Fig. 1D). In spite of this, the inverse correlation between PDK4 expression and MS4A1 expression was observed through Pearson correlation analysis (r = -0.41, P = 0.0021; Fig. 1E). In addition, the R-CHOP- resistant DLBCL cell line SU-DHL-2/R exhibited higher PDK4 than the R-CHOP-sensitive DLBCL cell line SU-DHL-2 at both the mRNA and protein levels, as did the rituximab-resistant DLBCL cell line OCI-ly8/R in comparison with rituximab-sensitive DLBCL cell line OCI-ly8 (Fig. 1F and 1G). The drug-resistance of the R-CHOP-resistant and rituximab-resistant DLBCL cell lines was identified by CCK-8 assay (Fig. S1A and 1B). Subsequently, immunofluorescence was performed to detect the expression of PDK4 and CD20 in R-CHOP-resistant DLBCL cells. It was revealed that the expression of PDK4 was elevated in SU-DHL-2/R relative to the parental cells, and that CD20 expression was downregulated for SU-DHL-2/R (Fig. 1H). These findings indicate the important role played by PDK4 in R-CHOP and rituximab resistance.

High PDK4 is associated with low MS4A1/CD20 and rituximab resistance in DLBCL cells

In order to figure out the potential role of PDK4 expression in rituximab resistance, there were three DLBCL cell lines, namely, U2932, OCI-ly7 and OCI-ly8 used for in vitro assays, including qRT-PCR, flow cytometry, and western blotting assays. A high consistence was observed between mRNA and protein expression for PDK4. In the meantime, U2932 exhibited the highest level of expression and OCI-ly7 is just the opposite (Fig. 2A and 2C). Consistently, there was an evident inverse correlation between PDK4 expression and MS4A1/CD20 expression (Fig. 2A – 2C) observed in these DLBCL cell lines. When these cell lines were treated with rituximab (50 μg/ml) for 48 hours, there was a negative relationship observed between PDK4 expression and rituximab sensitivity, as determined by the level of MS4A1/CD20 expression[40,41]. As shown in Figure 2D and 2E, the cell lines with low expression of PDK4 led to more significant apoptosis (19.79% ± 1.60% in OCI-ly7, 14.14% ± 1.96% in OCI-ly8) when compared with the high expression cell line (2.88% ± 1.02% in U2932; P < 0.001).

Targeting PDK4 increases rituximab sensitivity against DLBCL cells

In order to explore the effect of PDK4 on cell growth and rituximab resistance in DLBCL cells, there were two shRNA sequences (shRNA1 and shRNA2) targeting human PDK4 designed for this study. PDK4-deficient stable cell lines were generated using shRNAs (PDK4 sh1 and PDK4 sh2) in U2932 and OCI-ly8

cell lines, which reduced PDK4 protein expression significantly. Besides, a significant increase was observed in the percentage of apoptosis in transduced cells following rituximab treatment. According to Figure 3A and 3B, U2932: 5.96% ± 1.31%, PDK4 sh1 10.28% ± 1.03%, P = 0.012; PDK4 sh2 12.74% ± 2.20%, P = 0.011; and OCI-ly8: 13.32% ± 1.68%, PDK4 sh1 23.54% ± 2.25%, P = 0.0032; PDK4 sh2 21.21% ± 1.67%, P = 0.0045.

Due to the absence of specific modulator for PDK4, dichloroacetate (DCA), as a specific inhibitor of PDK4[42,43], was used to assess the impact of pharmacological PDK4 inhibition. Compared with rituximab alone, a significant increase of apoptosis was observed in cell lines when they were treated with rituximab (50 μg/mL) and DCA (5 mmol/L) for 48 hours (OCI-ly7: 20.25% ± 2.14% vs. 35.65% ± 3.87%, P = 0.0038; OCI-ly8: 13.63% ± 2.12% vs. 30.55% ± 3.39%, P = 0.0018), which is the case even in the U2932 cell line initially showing poor response to rituximab (5.54% ± 1.93% vs. 25.14% ± 3.66%, P = 0.0012; Fig. 3C). It is suggested that the PDK4 inhibitor DCA can be effective in reversing the rituximab resistance in DLBCL cells.

PDK4 has a negative regulatory effect on MS4A1/CD20 expression in DLBCL cells

PDK4 functions as a positive regulator of glycolysis during tumor development[25]. Rituximab performs its function through the ligation with cell surface CD20 molecule[44]. To further demonstrate the regulatory effect of PDK4 on MS4A1/CD20 in DLBCL cells, PDK4 was overexpressed by lentivirus in both U2932 and OCI-ly8 (Fig. 4A, 4B and 4F). As showing in Figure 4A and 4B, qRT-PCR analysis was conducted to confirm that the overexpression of PDK4 in U2932 and OCI-ly8 cells (P < 0.01) contributed to a reduction to MS4A1 mRNA levels (P < 0.05) accordingly. Through confocal microscopy, it was observed that the number of CD20 molecules located in the plasma membrane was signficantly reduced after the overexpression of PDK4 (PDK4 OE) as compared to the control (EV) both in U2932 and OCI-ly8 cells (Fig. 4C and 4D). Furthermore, the protein levels of CD20 improved with the deletion of PDK4 by shRNA (Fig. 4E) but declined with the overexpression of PDK4 by lentivirus (Fig. 4F). Moreover, according to the above-mentioned results, PDK4 knockdown increased rituximab sensitivity significantly which relied on the levels of MS4A1/CD20 expression[40,41]. To sum up, these results

demonstrate that PDK4 plays a negative role in regulating the expression of MS4A1/CD20 in DLBCL cells.

Rituximab resistant DLBCL cells showes a metabolic shift of active glycolysis and OXPHOS

In previous studies, it has been substantiated that there is metabolic heterogeneity in DLBCL[9,10]. Therefore, the metabolic profiles of SU-DHL-2/R and OCI-ly8/R cells were determined in this study. According to our data, the SU-DHL-2/R and OCI-ly8/R cells showed a significant increase in the level of glucose consumption (Fig. 5A) and the rate of lactate production (Fig. 5B) as compared to their parental cells. Moreover, the levels of extracellular ATP in SU-DHL-2/R and OCI-ly8/R cells were found to be significantly higher than in the parental cells (Fig. 5C).

Cells are capable of producing ATP through mitochondrial OXPHOS and glycolysis. In order to determine which was involved in the rituximab resistant cells, cellular oxidative phosphorylation and glycolysis were monitored by measuring the oxygen consumption rate (OCR) and extracellular acidification rate (ECAR) in real time. As suggested by the results, SU-DHL-2/R cells exhibited a significant increase in cellular OCR (Fig. 5E), suggesting an increase in the amount of ATP produced from mitochondrial OXPHOS in resistant cells as compared to the parental cells. According to seahorse analysis, SU-DHL-2/R cells led to an increase in ECAR, which means the overall glycolytic flux was higher than in the parental cells (Fig. 5D). To compare mitochondrial and non-mitochondrial in their contribution to the cellular energy budget, an assessment was conducted of the proportion of total cellular ATP with sensitivity to the inhibition of glycolysis versus mitochondrial metabolism[9]. Compared with the parental cells, the SU-DHL-2/R accounts for a significantly higher proportion of its total energy from glycolysis (~65%) than from mitochondrial oxidative metabolism (Fig. 5F), suggesting that the rituximab resistant cells had increased ATP production and glycolysis as compared to their parental cells.

PDK4 mediates the metabolic shift of rituximab resistant DLBCL cells

A further investigation was conducted into whether PDK4 was involved in the metabolic shift of rituximab resistant DLBCL cells. As suggested by the investigative results, the glucose consumption (Fig. 6A) and lactate production (Fig. 6B) of PDK4-deficient (PDK4 sh1) U2932 and OCI-ly8 cells were sharply reduced as compared to control cells. Accordingly, the extracellular ATP levels of PDK4-deficient cells also dropped when compared with control cells (Fig. 6C). According to seahorse analysis, the ECAR of PDK4-deficient cells diminished (Fig. 6D). However, the impact of PDK4-deficiency on metabolic features of U2932 cells was slightly reduced in OCI-ly8 cells (Fig. 6A – 6D), which is suspected to result from rituximab resistant cells being more reliant on glycolysis. These results demonstrate that PDK4 regulated the metabolic shift of rituximab resistant DLBCL cells.

Overexpression of PDK4 promotes proliferation and rituximab resistance in DLBCL cells

To ascertain whether or not high expression of PDK4 can promote cell growth and enhance rituximab resistance, a further study was conducted using the PDK4 overexpressing DLBCL cell lines U2932 and

OCI-ly8. As shown in Figure 7A, the capabilities of cell growth were significantly increased for PDK4 overexpressing OCI-ly8 cells as compared to controls after the treatment with rituximab (50 μg/ml) for 72 hours (P = 0.022). Subsequently, CCK-8 assay was performed using the PDK4 overexpressing U2932 and OCI-ly8 cells treated either with or without rituximab. U2932 (Fig. S2) and OCI-ly8 PDK4 overexpressing cells (Fig. 7B) exhibited a sharp increase in proliferative activity when compared with controls.

As confirmed by the aforementioned results, there was a knockdown of PDK4 sensitises DLBCL cells to rituximab *in vitro*. To verify this conclusion, it was further explored whether the overexpression of PDK4 could increase rituximab resistance in DLBCL cells *in vivo*. The xenograft mice model of DLBCL was constructed by subcutaneously transplanting PDK4 overexpressing OCI-ly8 cells into immunocompromised B-NDG mice, with the B-NDG mice transplanted with the same number of OCI-ly8 transfected with empty vector treated as controls. At day 10 after the injection of the DLBCL cells, half of the mice in both the PDK4 overexpressing group and empty vector group were treated with rituximab (12.5 mg/kg) injected intraperitoneal on a daily basis for 2 weeks. As shown in Figure 7C, 7D and 7F, the PDK4 overexpressing tumours developing in untreated mice were larger than the empty vector tumours (tumor weight: 0.042; tumor volume: P = 0.0034). However, there was no difference observed in body weight, indicating that the toxicity of rituximab treatment didn't reach a significant level (Fig. 7E). In addition, the xenografts with control vector showed significant tumor shrinkage after rituximab treatment, as indicated by tumor weight (P = 0.029) and tumor volume (P = 0.0019). In comparison, those with PDK4 overexpression showed significant reduction to neither tumor weight (P = 0.158) nor tumor volume (P = 0.083).

Discussion

At present, metabolic reprogramming has been regarded as a crucial marker of cancer progression, and identified as associated with drug resistance[20,45]. In this study, it was found out that PDK4 was overexpressed in rituximab resistant DLBCL cells. Then, it was further demonstrated that PDK4 promoted cell growth and enhanced rituximab resistance by mediating the metabolic shift in DLBCL cells. More importantly, our data suggested that PDK4 promoted rituximab resistance, at least in part, by regulating MS4A1/CD20 expression (Fig. 8).

Previously, it was proposed that the suppression of PDK4 can inhibit cell proliferation, increase apoptosis and regulate the sensitivity of drugs in solid tumors[20,22,46,47]. Moreover, PDK4 contributed to tumour progression in lung, cervical and liver cancers[20,25,47,48]. Therefore, it is suspected that PDK4 plays the role of an oncogene in the progression of cancer. In spite of this, the role of PDK4 in DLBCL remains unclear so far. In this study, an investigation was conducted into the role of PDK4 in rituximab-induced apoptosis and it was demonstrated that the reduction to PDK4 expression is correlated with rituximab sensibility in DLBCL. Moreover, the PDK4 inhibitor dichloroacetate is more effective in reversing rituximab resistance for the U2932 applied as rituximab-resistant DLBCL cell than OCI-ly7 and OCI-ly8. The inhibition of PDK4 expression or inhibitors of PDK4 hinders rituximab-induced apoptosis. The impact of PDK4 on DLBCL cell growth and rituximab resistance was further evidenced by the *in vitro* and *in vivo* data obtained to

suggest that PDK4 overexpressing tumours grow faster and are less responsive to the treatment of rituximab than tumours transfected with empty vector. In addition, it was also found out that PDK4 enhanced rituximab resistance in DLBCL cells. Therefore, PDK4 was identified as a potential target for DLBCL therapy.

The development of resistance to rituximab has been observed in DLBCL patients[17]. The repeated exposure to rituximab caused CD20 expression to decline gradually during the development of rituximab-resistant cell lines[18]. The down-modulation of CD20 expression after chemoimmunotherapy with rituximab contributed to rituximab resistance[18]. Recently, it has been reported that CD20-negative phenotypic change occurred to some (about 26.3%) of CD20-positive B-cell lymphoma patients after rituximab-based treatment[17]. However, the underlying mechanism of CD20-loss remains unknown. In some recent studies, it is proposed that both genetic and epigenetic mechanisms may be associated with the low levels of CD20 expression in newly diagnosed and relapsed/refractory DLBCL after the use of rituximab[16]. Epigenetic therapies, such as hypomethylating agent 5-aza-2'-deoxycytidine and histone deacetylase inhibitor (HDACi) chidamide, are effective in restoring both the cell surface expression of CD20 protein and rituximab sensitivity[17,19]. In other studies, an exploration was conducted into the regulatory mechanisms of CD20 expression. Rituximab resistance can result from any abnormality in the process of CD20 protein expression, such as downregulation, or alterations in the cell membrane[9,14,29]. In this study, it was discovered that PDK4 may perform a critical role in MS4A1/CD20 expression, because a lowered level of CD20 mRNA and protein was restored in the cells with PDK4 shRNAs while the mRNA and protein level of CD20 were reduced after the overexpression of PDK4 in DLBCL cells. Moreover, a negative relationship was observed between PDK4 expression and MS4A1/CD20. These results suggested that PDK4 could produce a negative regulatory effect on the expression of MS4A1/CD20 in DLBCL cells.

Metabolic reprogramming involves the overexpression of essential glycolytic enzymes, the acceleration of glycolytic flux, high-speed ATP production and the accumulation of lactate, which contributes significantly to tumor progression and the resistance to cancer therapy[49]. Tumor cells undergo metabolic alteration to fulfill the bioenergetic and biosynthetic needs for rapid cell proliferation[45]. As an important mitochondrial matrix enzyme for cellular energy regulation[50], PDK4 inhibits the entry of pyruvate into the TCA cycle, thus switching energy derivation to cytoplasmic glycolysis rather than mitochondrial OXPHOS[43,51]. Recently, DLBCL has been identified as a type of metabolic heterogeneity disease[9]. In this study, it was revealed that PDK4 was significantly elevated in rituximab-resistant DLBCL cells as compared to sensitive cells, suggesting that PDK4 upregulation is associated with rituximab resistance. To better understand the mechanisms of resistance to rituximab, several rituximab-resistant cell lines were investigated and characterized, with a metabolic shift observed, that is, the main energy source changed from OXPHOS to glycolysis as found out in the metabolic studies conducted using the Seahorse Bioanalyzer. Furthermore, our data suggested a metabolic signature of active glycolysis through the upregulation of PDK4. That is to say, PDK4 is involved in the regulation of glycolysis and rituximab sensitivity for DLBCL cells.

In a recent study, it was demonstrated that forced CD20 expression restored cytoplasmic rather than surface CD20, suggesting the existence of a defect in CD20 protein transport in rituximab-resistant cell lines[18]. Therefore, it was inferred in this study from the perspective of metabolism that, PDK4-mediated metabolic reprogramming could hinder the transport of CD20 protein from cytoplasm to cytomembrane. In a latest study, it was identified that GAPDH, a metabolic regulatory enzyme, can be relied on to predict the response of DLBCL patients to R-CHOP treatment and their sensitivity to specific metabolic inhibitors[10]. On this basis, it is sensible to judge that PDK4 may has a similar clinical significance for DLBCL. However, the survival and prognosis analysis of the patients was not conducted in this study for most patients still in follow-up. It is thus necessary to conduct further study in the future.

Conclusions

To sum up, this is the first study showing that the modulation of PDK4 can make difference to rituximab-induced cell apoptosis on DLBCL. Notably, a mechanism was discovered that PDK4 could promote proliferation and rituximab resistance in DLBCL cells through the mediation of metabolic reprogramming. PDK4 produces a negative regulatory effect on MS4A1/CD20 expression in DLBCL cells. This is the first study showing that targeting PDK4 has the potential to address the rituximab resistance in DLBCL. In order to find out about the novel mechanisms of CD20 downregulation in DLBCL, it is essential to conduct further studies on the relationship between PDK4-mediated metabolic reprogramming and CD20 protein transporting from cytoplasm to cytomembrane.

Abbreviations

ABC activated B-cell-like

ADCC antibody-dependent cellular cytotoxicity

CCC consensus cluster classification

CMC complement-dependent cytotoxicity

COO cell-of-origin

DCA dichloroacetate

DEGs the differentially expressed genes

DLBCL diffuse large B-cell lymphoma

ECAR extracellular acidification rate

GCB germinal-center B-cell-like

HDACi histone deacetylase inhibitor

OCR the oxygen consumption rate

OXPHOS oxidative phosphorylation

PDH pyruvate dehydrogenase complex

PDK4 pyruvate dehydrogenase lipoamide kinase isozyme 4

R-CHOP rituximab plus cyclophosphamide, doxorubicin, vincristine, and prednisone regimen

Declarations

Acknowledgments

The authors acknowledge Wang X.T, Guilin Medical University for editing the manuscript.

Authors' contributions

D.J. and Q.Z. designed experiments, analyzed data. D.J. and Q.M. performed experiments and wrote the paper. F.C. supervised the whole experiments. X.S. and G.Z. revised the paper. F.C. and Q.Z. supported the study. X.W. and M.D. edited the paper. The authors read and approved the final manuscript.

Funding

This work was supported by the National Natural Science Foundation of China (81570117); the National Natural Science Foundation of China (82060044); the Natural Science Foundation of Guangxi Province (2020GXNSFAA159018); the guiding project of Qinghai Provincial Health and Family Planning Commission (2018-wjzdx-17).

Availability of data and materials

Not applicable.

Ethics approval and consent to participate

Informed consent was obtained in accordance with the Declaration of Helsinki. All laboratory experiments with primary samples and animal procedures were reviewed and approved by the Medical Ethics Committee of the Third Xiangya Hospital, Central South University.

Consent for publication

All authors have agreed to the publication of this manuscript.

Competing interests

The authors declare no conflicts of interest in this work.

Contributor Information

Qiangqiang Zhao, Email: zgxyws@163.com.

References

1. Sukswai N, Lyapichev K, Khoury JD, Medeiros LJ. Diffuse large B-cell lymphoma variants: an update. Pathology. 2020;52(1):53–67. doi:10.1016/j.pathol.2019.08.013.
2. Liu Y, Barta SK. Diffuse large B-cell lymphoma: 2019 update on diagnosis, risk stratification, and treatment. Am J Hematol. 2019;94(5):604–16. doi:10.1002/ajh.25460.
3. Herrera AF, et al. Relapsed or Refractory Double-Expressor and Double-Hit Lymphomas Have Inferior Progression-Free Survival After Autologous Stem-Cell Transplantation. J Clin Oncol. 2017;35(1):24–31. doi:10.1200/JCO.2016.68.2740.
4. Hu S, et al. MYC/BCL2 protein coexpression contributes to the inferior survival of activated B-cell subtype of diffuse large B-cell lymphoma and demonstrates high-risk gene expression signatures: a report from The International DLBCL Rituximab-CHOP Consortium Program. Blood. 2013;121(20):4021–31. doi:10.1182/blood-2012-10-460063. quiz 4250.
5. Vardhana SA, et al. Outcomes of primary refractory diffuse large B-cell lymphoma (DLBCL) treated with salvage chemotherapy and intention to transplant in the rituximab era. Br J Haematol. 2017;176(4):591–9. doi:10.1111/bjh.14453.
6. Susanibar-Adaniya S, Barta SK. 2021 Update on Diffuse large B cell lymphoma: A review of current data and potential applications on risk stratification and management. Am J Hematol. 2021; **96**(5): 617–629. doi: 10.1002/ajh.26151.
7. Schmitz R, et al. Genetics and Pathogenesis of Diffuse Large B-Cell Lymphoma. N Engl J Med. 2018;378(15):1396–407. doi:10.1056/NEJMoa1801445.
8. Monti S, et al. Molecular profiling of diffuse large B-cell lymphoma identifies robust subtypes including one characterized by host inflammatory response. Blood. 2005;105(5):1851–61. doi:10.1182/blood-2004-07-2947.
9. Caro P, et al. Metabolic signatures uncover distinct targets in molecular subsets of diffuse large B cell lymphoma. Cancer Cell. 2012;22(4):547–60. doi:10.1016/j.ccr.2012.08.014.
10. Chiche J, et al. GAPDH Expression Predicts the Response to R-CHOP, the Tumor Metabolic Status, and the Response of DLBCL Patients to Metabolic Inhibitors. Cell Metab. 2019;29(6):1243–57. . doi: 10.1016/j.cmet.2019.02.002.
11. Smith MR. Rituximab (monoclonal anti-CD20 antibody): mechanisms of action and resistance. Oncogene. 2003;22(47):7359–68. doi:10.1038/sj.onc.1206939.
12. Pérez-Callejo D, González-Rincón J, Sánchez A, Provencio M, Sánchez-Beato M. Action and resistance of monoclonal CD20 antibodies therapy in B-cell Non-Hodgkin Lymphomas. Cancer Treat Rev. 2015;41(8):680–9. doi:10.1016/j.ctrv.2015.05.007.

13. Deans JP, Li H, Polyak MJ. CD20-mediated apoptosis: signalling through lipid rafts. Immunology. 2002;107(2):176–82. doi:10.1046/j.1365-2567.2002.01495.x.
14. Zou L, et al. Mechanism and Treatment of Rituximab Resistance in Diffuse Large Bcell Lymphoma. Curr Cancer Drug Targets. 2019;19(9):681–7. doi:10.2174/1568009619666190126125251.
15. Rushton CK, et al. Genetic and evolutionary patterns of treatment resistance in relapsed B-cell lymphoma. Blood Adv. 2020;4(13):2886–98. doi:10.1182/bloodadvances.2020001696.
16. Tomita A. Genetic and Epigenetic Modulation of CD20 Expression in B-Cell Malignancies: Molecular Mechanisms and Significance to Rituximab Resistance. J Clin Exp Hematop. 2016;56(2):89–99. doi:10.3960/jslrt.56.89.
17. Hiraga J, et al. Down-regulation of CD20 expression in B-cell lymphoma cells after treatment with rituximab-containing combination chemotherapies: its prevalence and clinical significance. Blood. 2009;113(20):4885–93. doi:10.1182/blood-2008-08-175208.
18. Tsai PC, Hernandez-Ilizaliturri FJ, Bangia N, Olejniczak SH, Czuczman MS. Regulation of CD20 in rituximab-resistant cell lines and B-cell non-Hodgkin lymphoma. Clin Cancer Res. 2012;18(4):1039–50. doi:10.1158/1078-0432.CCR-11-1429.
19. Guan XW, et al. Novel HDAC inhibitor Chidamide synergizes with Rituximab to inhibit diffuse large B-cell lymphoma tumour growth by upregulating CD20. Cell Death Dis. 2020;11(1):20. doi:10.1038/s41419-019-2210-0.
20. Zhao Z, Ji M, Wang Q, He N, Li Y. miR-16-5p/PDK4-Mediated Metabolic Reprogramming Is Involved in Chemoresistance of Cervical Cancer. Mol Ther Oncolytics. 2020;17:509–17. doi:10.1016/j.omto.2020.05.008.
21. Wu X, et al. Phosphoglycerate dehydrogenase promotes proliferation and bortezomib resistance through increasing reduced glutathione synthesis in multiple myeloma. Br J Haematol. 2020;190(1):52–66. doi:10.1111/bjh.16503.
22. Wang J, Qian Y, Gao M. Overexpression of PDK4 is associated with cell proliferation, drug resistance and poor prognosis in ovarian cancer. Cancer Manag Res. 2018;11:251–62. doi:10.2147/CMAR.S185015.
23. Guda MR, et al. Targeting PDK4 inhibits breast cancer metabolism. Am J Cancer Res. 2018; **8**(9): 1725–1738. eCollection 2018.
24. Woolbright BL, et al. The Role of Pyruvate Dehydrogenase Kinase-4 (PDK4) in Bladder Cancer and Chemoresistance. Mol Cancer Ther. 2018;17(9):2004–12. doi:10.1158/1535-7163.MCT-18-0063.
25. Li Z, et al. N^6-methyladenosine regulates glycolysis of cancer cells through PDK4. Nat Commun. 2020;11(1):2578. doi:10.1038/s41467-020-16306-5.
26. Stacpoole PW. Therapeutic Targeting of the Pyruvate Dehydrogenase Complex/Pyruvate Dehydrogenase Kinase (PDC/PDK) Axis in Cancer. J Natl Cancer Inst 2017; 109(11). doi:10.1093/jnci/djx071.

27. Sabattini E, Bacci F, Sagramoso C, Pileri SA. WHO classification of tumours of haematopoietic and lymphoid tissues in 2008: an overview. Pathologica. 2010;102(3):83–7.
28. Feng Y, et al. Exosome-derived miRNAs as predictive biomarkers for diffuse large B-cell lymphoma chemotherapy resistance. Epigenomics. 2019;11(1):35–51. doi:10.2217/epi-2018-0123.
29. Czuczman MS, et al. Acquirement of rituximab resistance in lymphoma cell lines is associated with both global CD20 gene and protein down-regulation regulated at the pretranscriptional and posttranscriptional levels. Clin Cancer Res. 2008;14(5):1561–70. doi:10.1158/1078-0432.CCR-07-1254.
30. Liang H, et al. Targeting the PI3K/AKT pathway via GLI1 inhibition enhanced the drug sensitivity of acute myeloid leukemia cells. Sci Rep. 2017;7:40361. doi:10.1038/srep40361.
31. Trapnell C, et al. Differential gene and transcript expression analysis of RNA-seq experiments with TopHat and Cufflinks. Nat Protoc. 2012;7(3):562–78. doi:10.1038/nprot.2012.016.
32. Zhai S, Zhao L, Lin T, Wang W. Downregulation of miR-33b promotes non-small cell lung cancer cell growth through reprogramming glucose metabolism miR-33b regulates non-small cell lung cancer cell growth. J Cell Biochem. 2019;120(4):6651–60. doi:10.1002/jcb.27961.
33. Shepherd RK, et al. Measurement of ATP production in mitochondrial disorders. J Inherit Metab Dis. 2006;29(1):86–91. doi:10.1007/s10545-006-0148-8.
34. Guppy M, Leedman P, Zu X, Russell V. Contribution by different fuels and metabolic pathways to the total ATP turnover of proliferating MCF-7 breast cancer cells. Biochem J. 2002;364(Pt 1):309–15. doi:10.1042/bj3640309.
35. Sun S, et al. R406 elicits anti-Warburg effect via Syk-dependent and -independent mechanisms to trigger apoptosis in glioma stem cells. Cell Death Dis. 2019;10(5):358. doi:10.1038/s41419-019-1587-0.
36. Chen R, et al. Sequential treatment with aT19 cells generates memory CAR-T cells and prolongs the lifespan of Raji-B-NDG mice. Cancer Lett. 2020;469:162–72. doi:10.1016/j.canlet.2019.10.022.
37. Xiao X, et al. Identification of 11(13)-dehydroivaxillin as a potent therapeutic agent against non-Hodgkin's lymphoma. Cell Death Dis. 2017;8(9):e3050. doi:10.1038/cddis.2017.442.
38. Gong J, et al. Preliminary biological evaluation of 123I-labelled anti-CD30-LDM in CD30-positive lymphomas murine models. Artif Cells Nanomed Biotechnol. 2020;48(1):408–14. doi:10.1080/21691401.2019.1709857.
39. Cheson BD, et al. Recommendations for initial evaluation, staging, and response assessment of Hodgkin and non-Hodgkin lymphoma: the Lugano classification. J Clin Oncol. 2014;32(27):3059–68. doi:10.1200/JCO.2013.54.8800.
40. van Meerten T, van Rijn RS, Hol S, Hagenbeek A, Ebeling SB. Complement-induced cell death by rituximab depends on CD20 expression level and acts complementary to antibody-dependent cellular cytotoxicity. Clin Cancer Res. 2006;12(13):4027–35.
41. Bil J, et al. Bortezomib modulates surface CD20 in B-cell malignancies and affects rituximab-mediated complement-dependent cytotoxicity. Blood. 2010;115(18):3745–55. doi:10.1182/blood-

2009-09-244129.

42. Fekir K, et al. Retrodifferentiation of Human Tumor Hepatocytes to Stem Cells Leads to Metabolic Reprogramming and Chemoresistance. Cancer Res. 2019;79(8):1869–83. doi:10.1158/0008-5472.CAN-18-2110.
43. Ma WQ, Sun XJ, Zhu Y, Liu NF. PDK4 promotes vascular calcification by interfering with autophagic activity and metabolic reprogramming. Cell Death Dis. 2020;11(11):991. doi:10.1038/s41419-020-03162-w.
44. Bojarczuk K, et al. B-cell receptor pathway inhibitors affect CD20 levels and impair antitumor activity of anti-CD20 monoclonal antibodies. Leukemia. 2014;28(5):1163–7. doi:10.1038/leu.2014.12.
45. Biswas SK. Metabolic Reprogramming of Immune Cells in Cancer Progression. Immunity. 2015;43(3):435–49. doi:10.1016/j.immuni.2015.09.001.
46. Leclerc D, et al. Oncogenic role of PDK4 in human colon cancer cells. Br J Cancer. 2017;116(7):930–6. doi:10.1038/bjc.2017.38.
47. Yu S, et al. PDK4 promotes tumorigenesis and cisplatin resistance in lung adenocarcinoma via transcriptional regulation of EPAS1. Cancer Chemother Pharmacol. 2021;87(2):207–15. doi:10.1007/s00280-020-04188-9.
48. Li G, et al. The microRNA-182-PDK4 axis regulates lung tumorigenesis by modulating pyruvate dehydrogenase and lipogenesis. Oncogene. 2017;36(7):989–98. doi:10.1038/onc.2016.265.
49. Vaupel P, Schmidberger H, Mayer A. The Warburg effect: essential part of metabolic reprogramming and central contributor to cancer progression. Int J Radiat Biol. 2019;95(7):912–9. doi:10.1080/09553002.2019.1589653.
50. Jeong JY, Jeoung NH, Park KG, Lee IK. Transcriptional regulation of pyruvate dehydrogenase kinase. Diabetes Metab J. 2012;36(5):328–35. doi:10.4093/dmj.2012.36.5.328.
51. Li X, et al. Mitochondria-Translocated PGK1 Functions as a Protein Kinase to Coordinate Glycolysis and the TCA Cycle in Tumorigenesis. Mol Cell. 2016;61(5):705–19. doi:10.1016/j.molcel.2016.02.009.

Figures

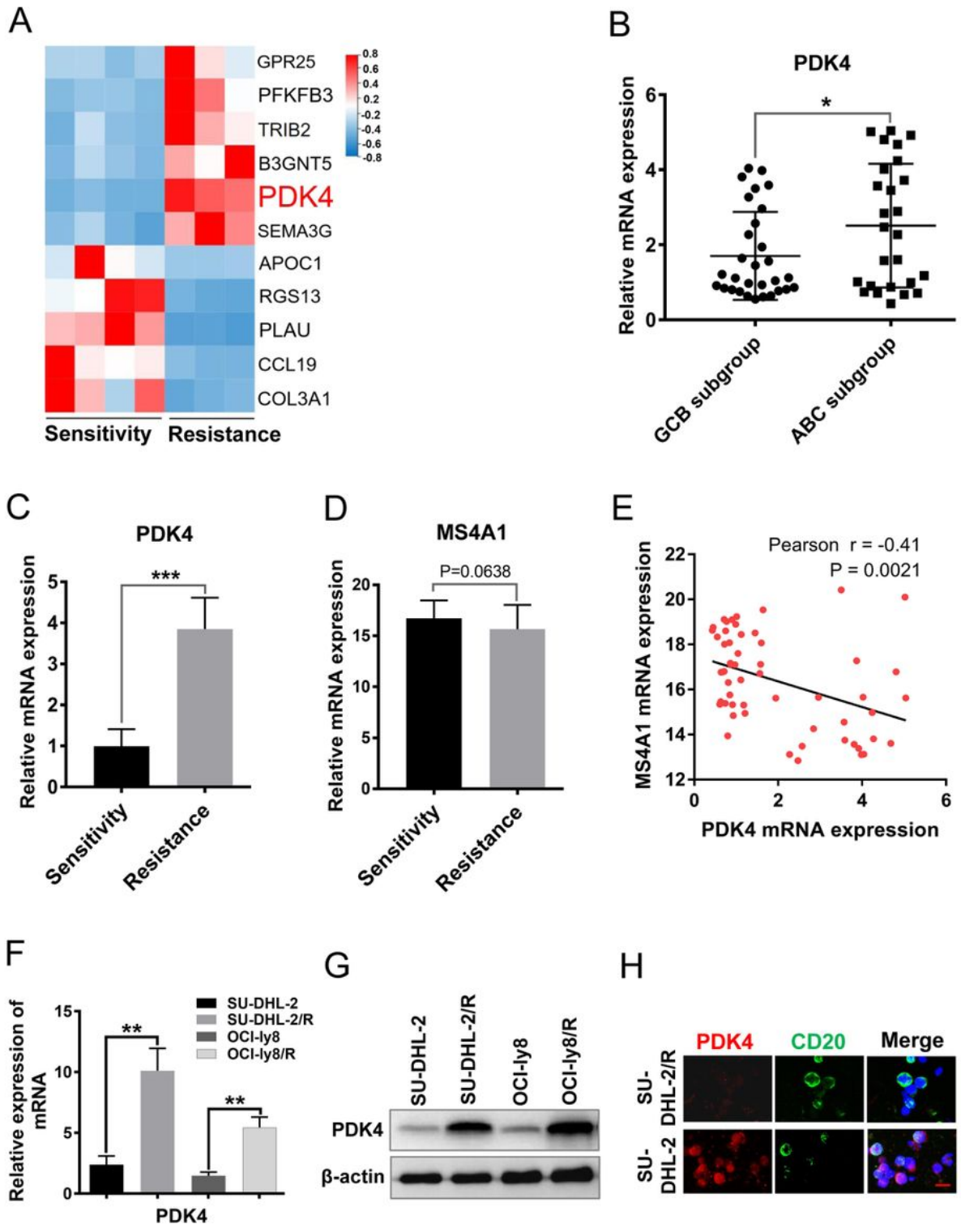

Figure 1

High PDK4 is associated with R-CHOP resistance in DLBCL cells. A, Gene expression detected by RNA-Seq and expression of PDK4 in DLBCL patients. Hierarchical cluster analysis of the top 11 deregulated genes in R-CHOP-sensitive patients (n = 4) and R-CHOP-resistance patients (n = 3). Upregulated genes are shown in red and downregulated genes are shown in blue. B, In the 56 cases of DLBCL cohort, PDK4 mRNA expression between GCB-DLBCL (n = 30) and ABC-DLCBL (n = 26) subtypes (* P<0.05, with t test).

C and D, qRT-PCR analysis of PDK4 mRNA (*** P<0.001, with Mann-Whitney U test) and MS4A1 mRNA (NS P > 0.05, with t test) expression in R-CHOP-sensitive patients (n = 37) and R-CHOP-resistant patients (n = 19) with DLBCL. E, Pearson correlation analysis for PDK4 and MS4A1 expression in the 56 cases of DLBCL cohort (Pearson r = -0.41, P = 0.0021, with F test). F and G, Assessment of both mRNA and protein levels of PDK4 in R-CHOP-resistant DLBCL cell line SU-DHL-2/R and rituximab-resistant DLBCL cell line OCI-ly8/R, as well as their parental cell lines. H, Representative images of immunofluorescence analysis for PDK4 (Red) and CD20 (Green) protein expression in SU-DHL-2/R and the parental cells. Scale bars represent 15 μm.

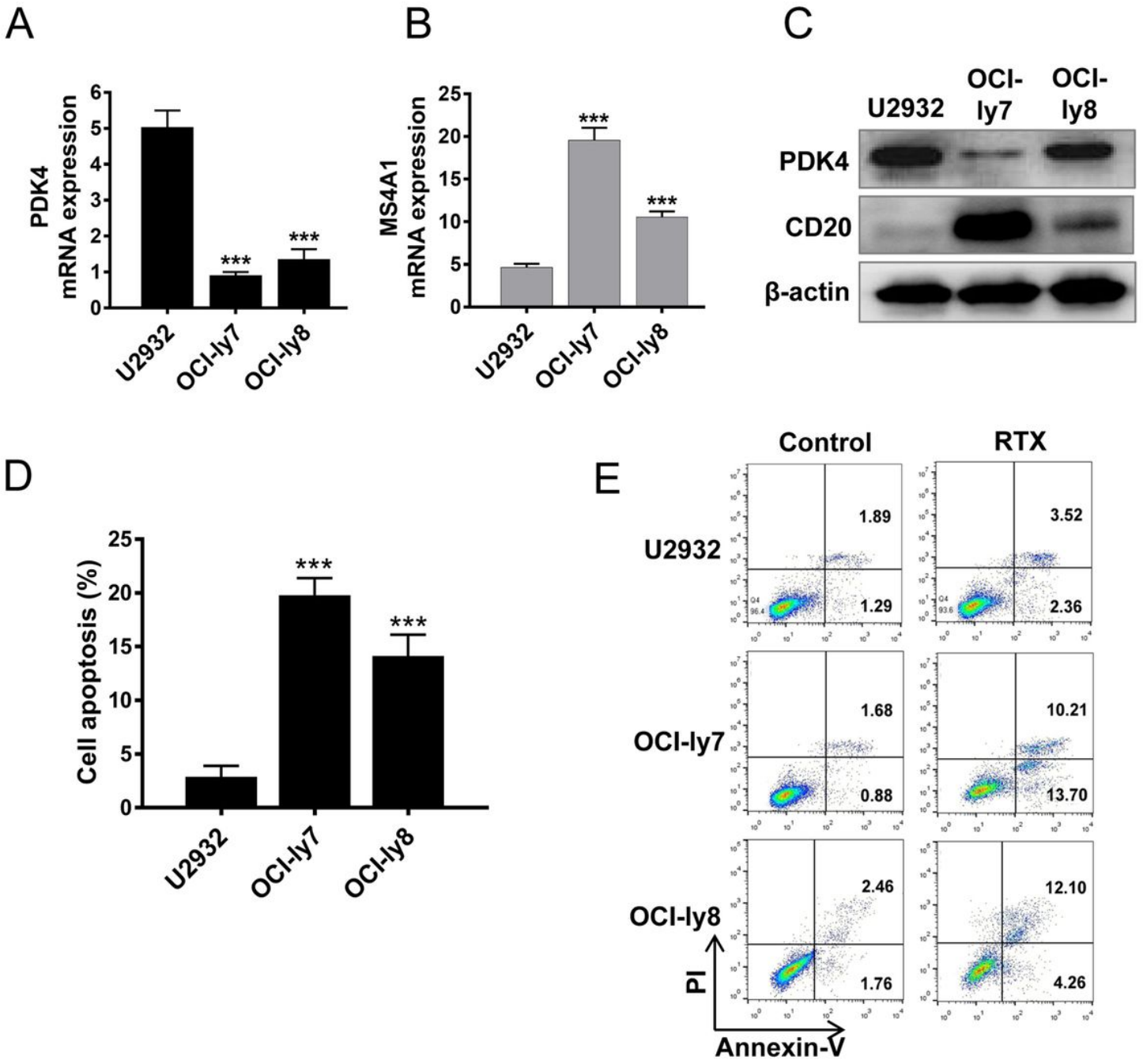

Figure 2

High PDK4 is associated with rituximab (RTX) resistance and low MS4A1/CD20 in DLBCL cells. A and B, qRT-PCR analysis of PDK4 and MS4A1 mRNA expression in DLBCL cell lines U2932, OCI-ly7 and OCI-ly8. C, western blotting analysis of PDK4 and CD20 protein levels in DLBCL cell lines U2932, OCI-ly7 and OCI-ly8. D and E, annexin V-FITC/PI double staining analysis of the three DLBCL cell lines treated with rituximab (50 μg/ml). n = 3, compared with U2932: *** P<0.001, with t test.

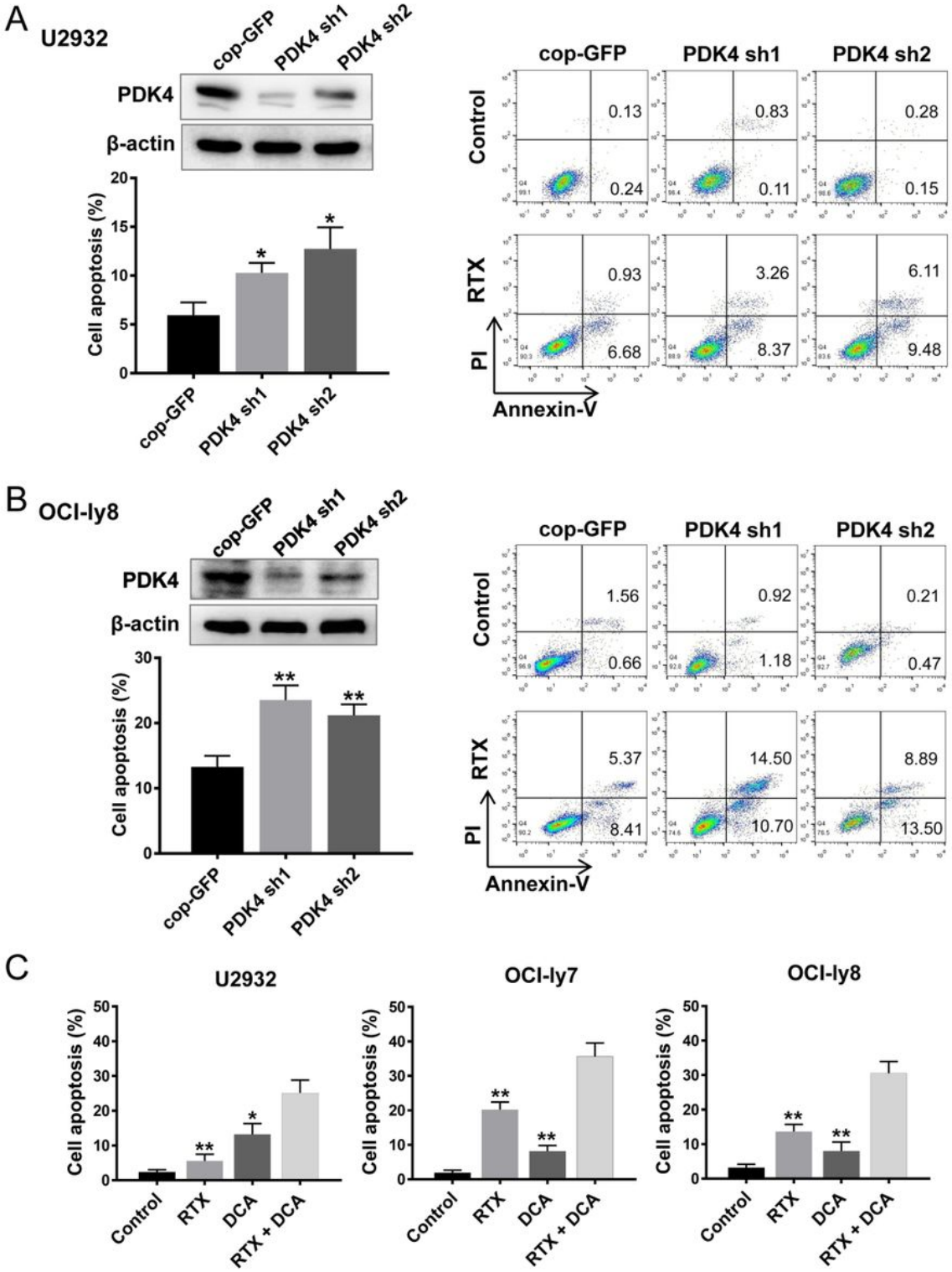

Figure 3

Inhibition of PDK4 by shRNA or dichloroacetate (DCA) sensitizes DLBCL cells to rituximab (RTX). A and B, annexin V-FITC/PI double staining analysis of DLBCL cells treated with rituximab (50 μg/ml) . The interference with shRNA to PDK4 increased the percentage of rituximab-induced cell apoptosis in U2932 and OCI-Ly8 cell line. n = 3, compared with cop-GFP: * P < 0.05, with t test. C, The PDK4 inhibitor dichloroacetate (DCA) enhanced the rituximab-induced apoptosisin DLBCL cell lines U2932, OCI-ly7 and OCI-Ly8. n = 3, compared with RTX (50 μg/ml) + DCA (5 mM): * P<0.05, ** P<0.01, with t test.

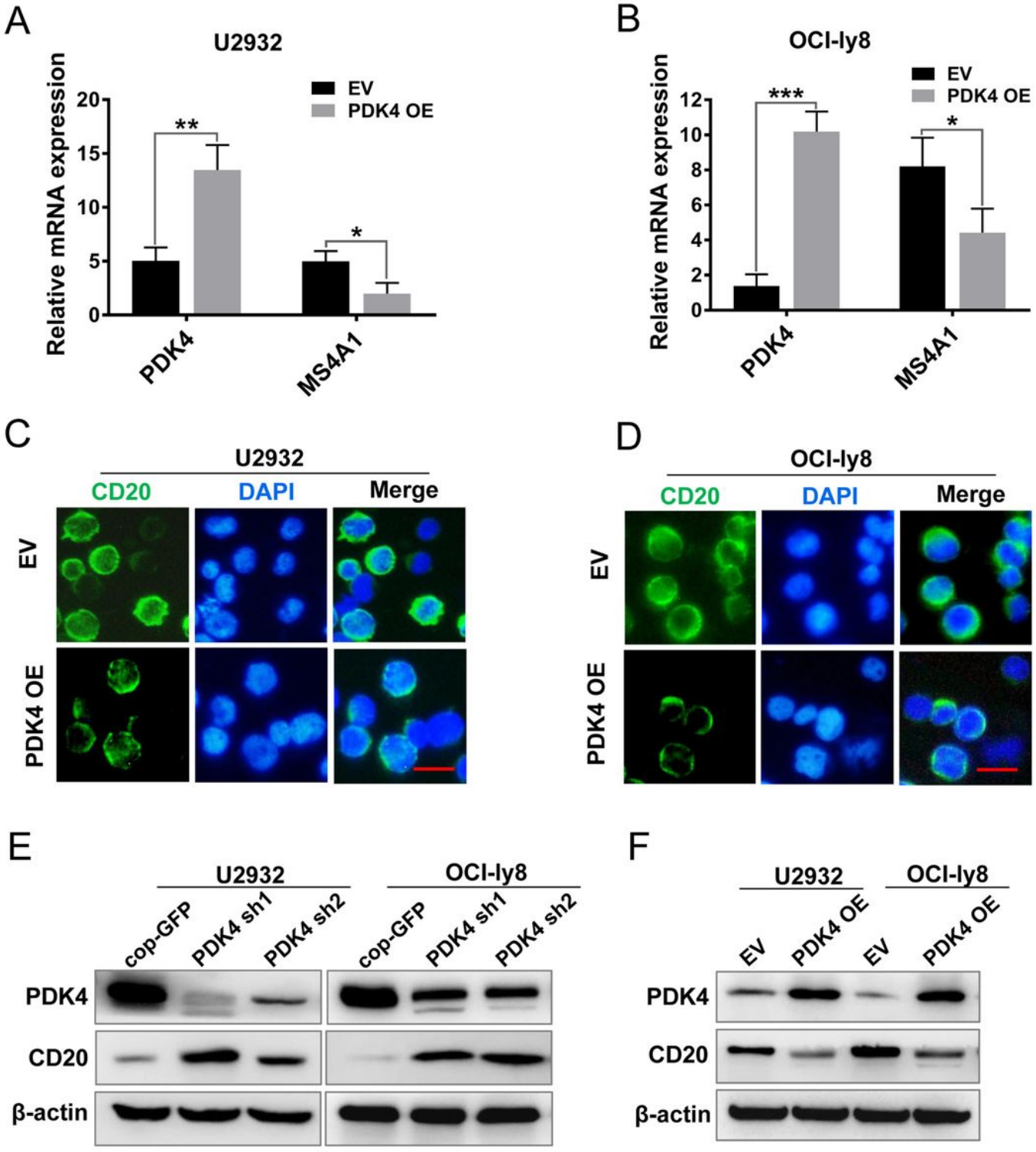

Figure 4

PDK4 has a negative regulatory effect on MS4A1/CD20 expression in DLBCL cells. A and B, qRT-PCR analysis of PDK4 and MS4A1 mRNA expression in U2932 and OCI-Ly8 cells transfected with PDK4 overexpressing (PDK4 OE) plasmid or empty vector (PDK4 EV). n = 3, compared with PDK4 EV: * $P < 0.05$, ** $P < 0.01$, *** $P < 0.001$, with t test. C and D, CD20 (green) molecules in the plasma membrane exhibited a reduction after PDK4 overexpression in both U2932 and OCI-Ly8 cells. Scale bars represent 15 μm. E and F, western blotting analysis of PDK4 and CD20 protein levels in U2932 and OCI-Ly8 cells interfered with shRNA to PDK4 or transfected with PDK4 overexpressing (PDK4 OE) plasmid, as well as their vector control.

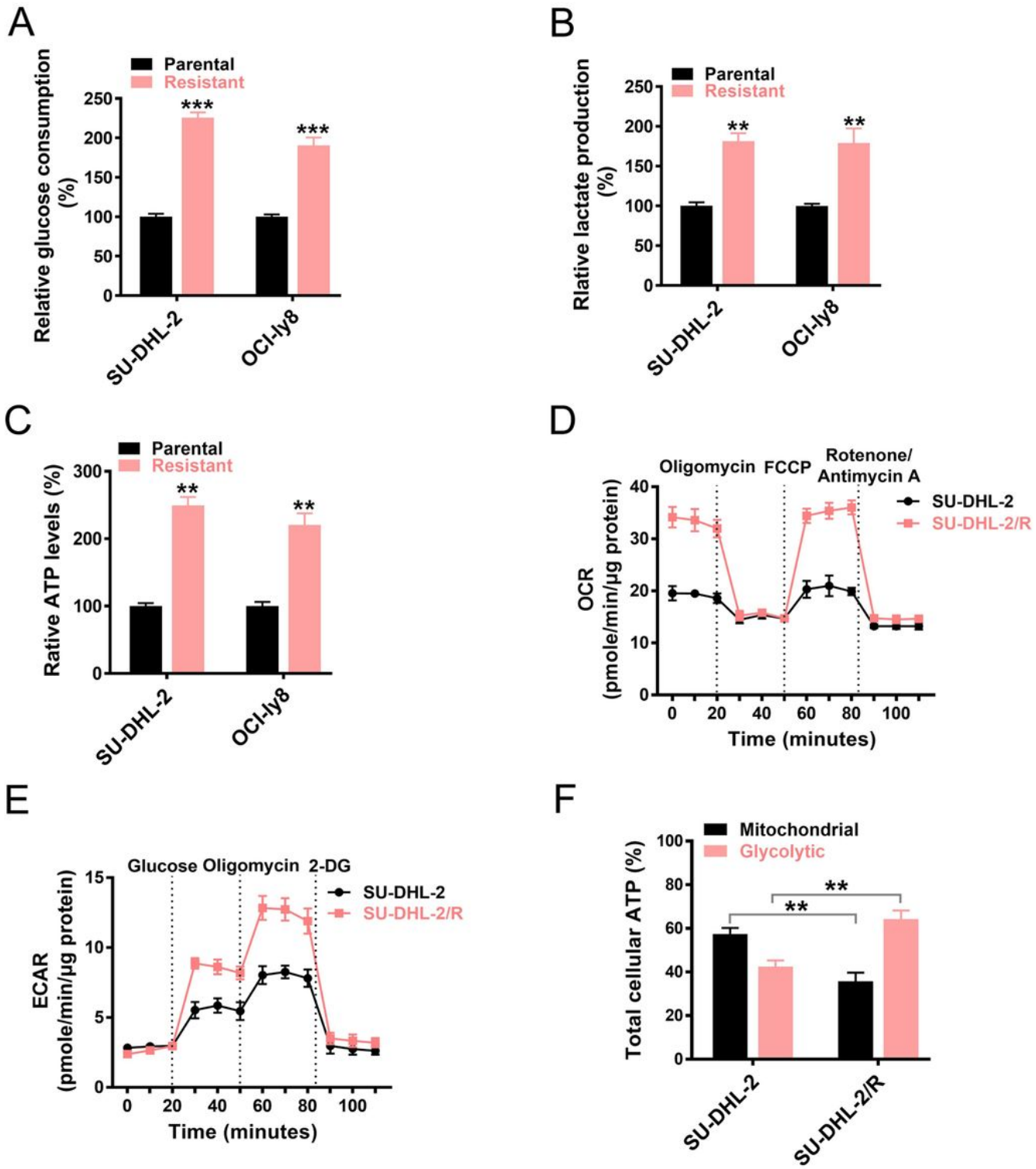

Figure 5

Rituximab resistant DLBCL cells showes a metabolic shift of active glycolysis and OXPHOS. A - C, The glucose consumption (A), lactate production (B), and ATP levels (C) in RCHOP-resistant DLBCL cell line SU-DHL-2/R and rituximab-resistant DLBCL cell line OCI-ly8/R, as well as their parental cell lines. n = 3, compared with parental: ** P < 0.01, *** P < 0.001, with t test. D and E, The cellular OCR (D) or ECAR (E) of SU-DHL-2/R and SU-DHL-2 cells was determined. F, Percent contribution of glycolysis and mitochondrial

metabolism to total cellular ATP of SU-DHL-2/R and the parental cells according to energy budget calculations. n = 3, compared with the parental cell line SU-DHL-2: ** P < 0.01, with t test.

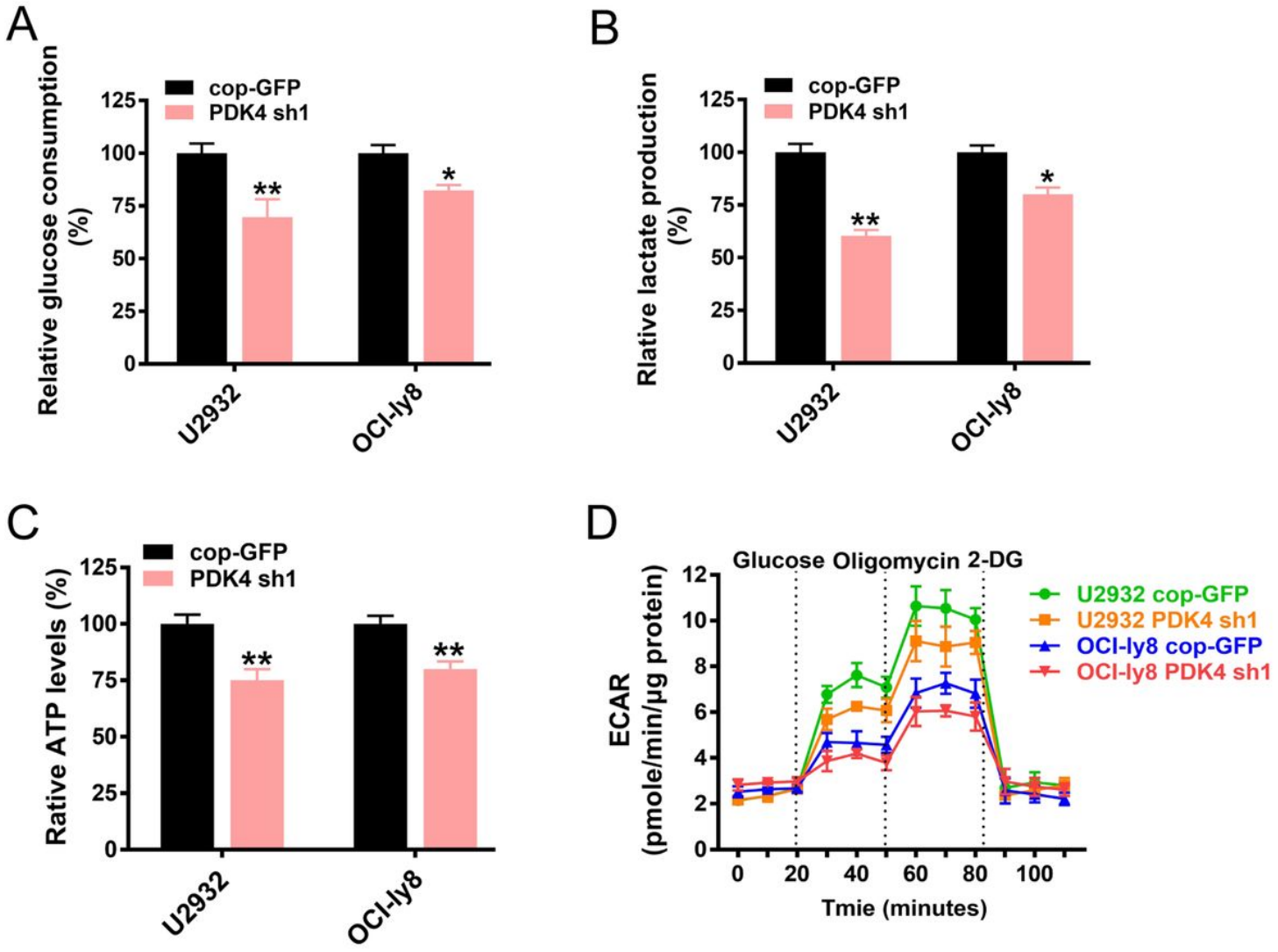

Figure 6

PDK4 mediates the metabolic shift of rituximab resistant DLBCL cells. A - D, U2932 and OCI-ly8 cells were transfected with cop-GFP or interfered shRNA on PDK4 (PDK4-sh1), the glucose consumption (A), lactate production (B), ATP levels (C), and cellular ECAR (D) were measured.

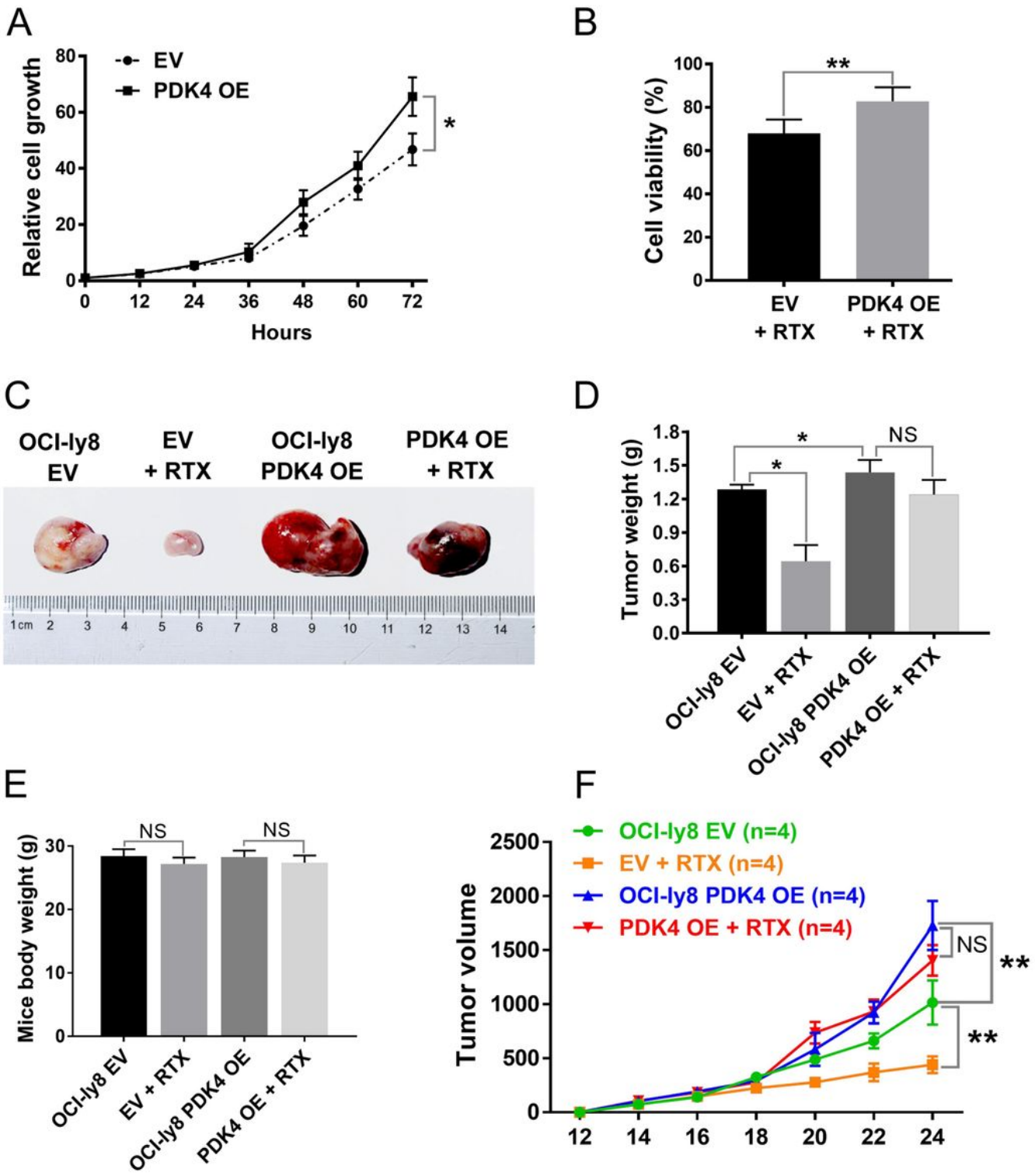

Figure 7

Overexpression of PDK4 promotes proliferation and rituximab resistance in DLBCL cells. A, In vitro cell growth assay showing relative cell growth curves of OCI-Ly8 empty vector (EV) and OCI-Ly8 PDK4 overexpressing (OE) cells treated with rituximab (50 μg/ml) for indicated time (n = 6, * P < 0.05, with one-way ANOVA). B, OCI-Ly8 EV and PDK4 OE cells were treated with rituximab (50 μg/ml) for 48 hours, the cell viability rate were analysed using CCK-8 assays (n = 6, * P < 0.05, with t test). C, D and F, in vivo

xenograft mice models of PDK4 overexpressing OCI-ly8 cells (OCI-ly8 PDK4 OE) or OCI-ly8 cells transfected with empty vector (OCI-ly8 EV) treated with rituximab (12.5 mg/kg) or PBS. Differences in tumour weight (D) and tumour volume (F) are shown between those four groups (n = 4, NS P > 0.05; * P < 0.05; ** P < 0.01; with t test). E, body weight of mice in each experimental group measured at day 24 (n = 4, compared with rituximab untreated group, NS P > 0.05, with t test).

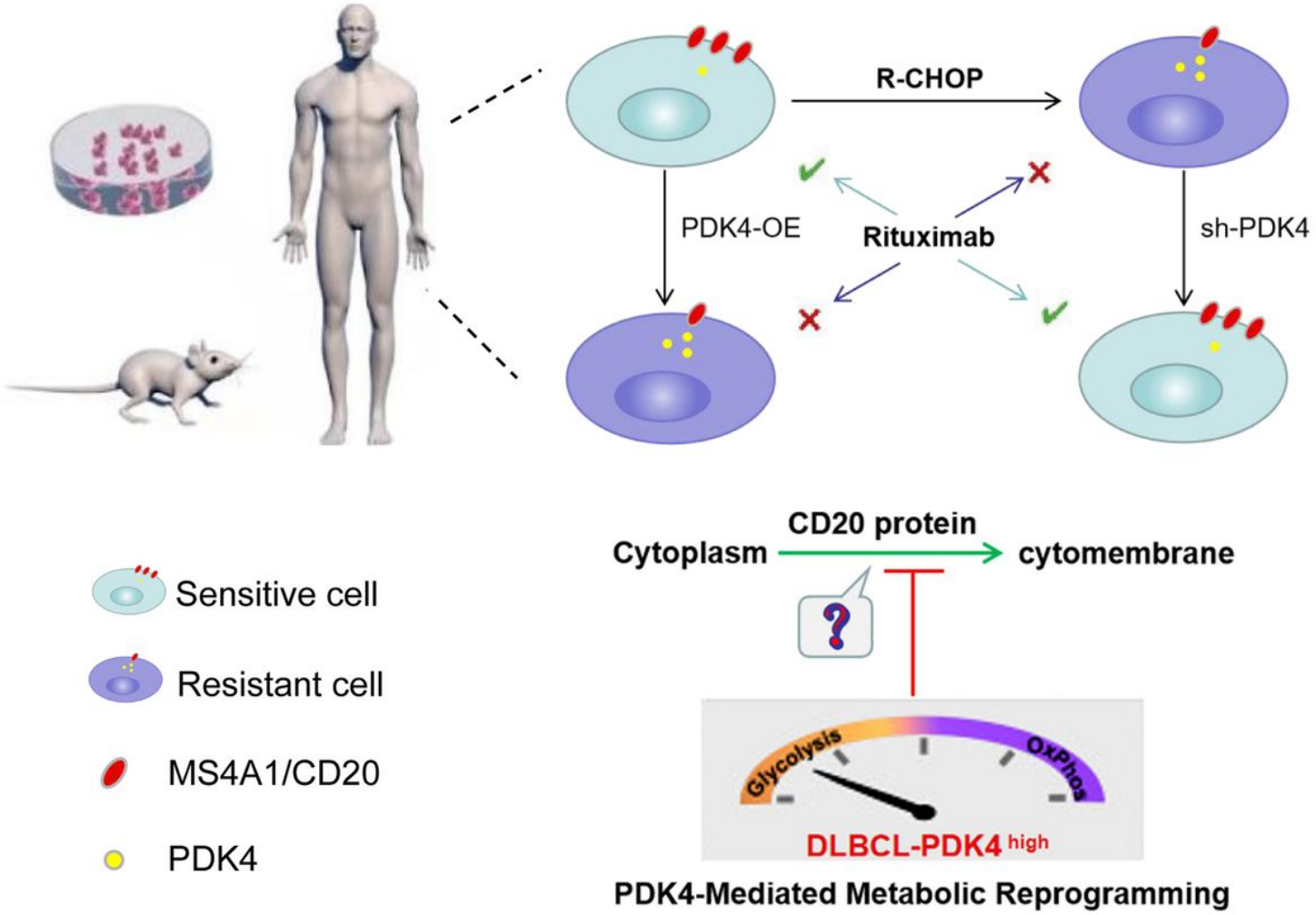

Figure 8

The model of our working hypothesis.

Supplementary Files

This is a list of supplementary files associated with this preprint. Click to download.

- SupplementaryMaterials.doc